CrossMark

ORIGINAL PAPER

Comparative assessment of spatiotemporal snow cover changes and hydrological behavior of the Gilgit, Astore and Hunza River basins (Hindukush–Karakoram–Himalaya region, Pakistan)

Adnan Ahmad Tahir[1,2] · Jan Franklin Adamowski[3] · Pierre Chevallier[4] · Ayaz Ul Haq[1] · Silvia Terzago[5]

Abstract The Upper Indus Basin (UIB), situated in the Himalaya–Karakoram–Hindukush (HKH) mountain ranges, is the major contributor to the supply of water for irrigation in Pakistan. Improved management of downstream water resources requires studying and comparing spatiotemporal changes in the snow cover and hydrological behavior of the river basins located in the HKH region. This study explored in detail the recent changes that have occurred in the Gilgit River basin (12,656 km^2; western sub-basin of UIB), which is characterized by a mean catchment elevation of 4250 m above sea level (m ASL). The basin's snow cover was monitored through the snow products provided by the MODIS satellite sensor, while analysis of its hydrological regime was supported by hydrological and climatic data recorded at different altitudes. The Gilgit basin findings were compared to those previously obtained for the lower-altitude Astore basin (mean catchment elevation = 4100 m ASL) and the higher-altitude Hunza basin (mean catchment elevation = 4650 m ASL). These three catchments were selected because of their different glacier coverage, contrasting area distribution at high altitudes and significant impact on the Upper Indus River flow. Almost 7, 5 and 33 % of the area of the Gilgit, Astore and Hunza basins, respectively, are situated above 5000 m ASL, and approximately 8, 6 and 25 %, respectively, are covered by glaciers. The UIB region was found to follow a stable or slightly increasing trend in snow coverage and had a discharge dominated by snow and glacier melt in its western (Hindukush–Karakoram), southern (Western-Himalaya) and northern (Central-Karakoram) sub-basins.

Responsible Editor: S.-W. Kim.

✉ Adnan Ahmad Tahir
uaf_adnan@hotmail.fr

Jan Franklin Adamowski
jan.adamowski@mcgill.ca

Pierre Chevallier
pierre.chevallier@ird.fr

Ayaz Ul Haq
ayazulhaq86@gmail.com

Silvia Terzago
s.terzago@isac.cnr.it

[1] Department of Environmental Sciences, COMSATS Institute of Information Technology, 22060 Abbottabad, Pakistan

[2] Institute of Earth Surface Dynamics, Faculty of Geosciences and Environment, University of Lausanne, Lausanne, Switzerland

[3] Department of Bioresource Engineering, McGill University, Ste Anne de Bellevue, QC H9X3V9, Canada

[4] Université de Montpellier, Laboratoire Hydrosciences (CNRS, IRD, Université de Montpellier), CC57, 163, rue Auguste Broussonnet, 34090 Montpellier, France

[5] Institute of Atmospheric Sciences and Climate (ISAC), National Research Council, Corso Fiume 4, 10133 Turin, Italy

1 Introduction and background

Pakistan's agriculture-based economy is dependent on irrigation waters supplied by the Indus River and its tributaries (SIHP 1990). Channeled through the Upper Indus Basin (UIB), most of the Indus River flow at Tarbela is comprised of snow and glacier melt (Bookhagen and Burbank 2010; Immerzeel et al. 2012, 2013; Mukhopadhyay and Khan 2014a) originating from the Himalaya–Karakoram–Hindukush mountains (Fig. 1a). The Tarbela reservoir, constructed on the Indus River, supplies
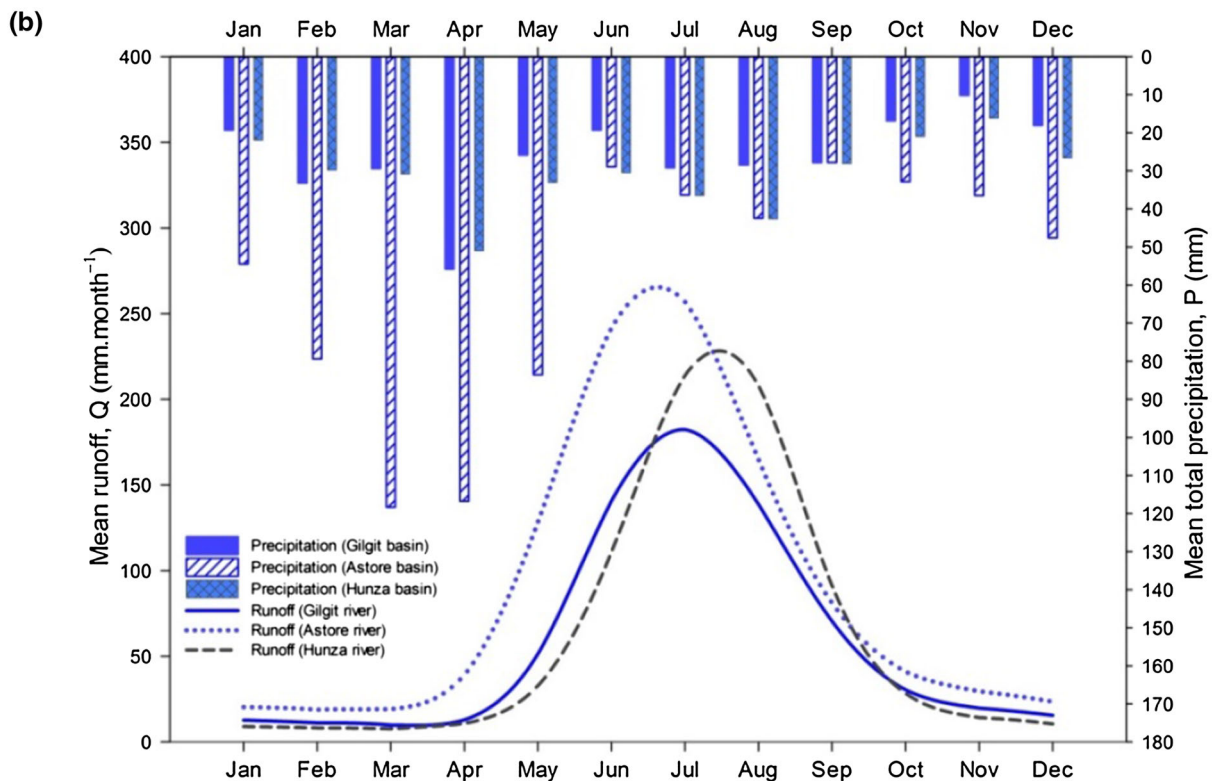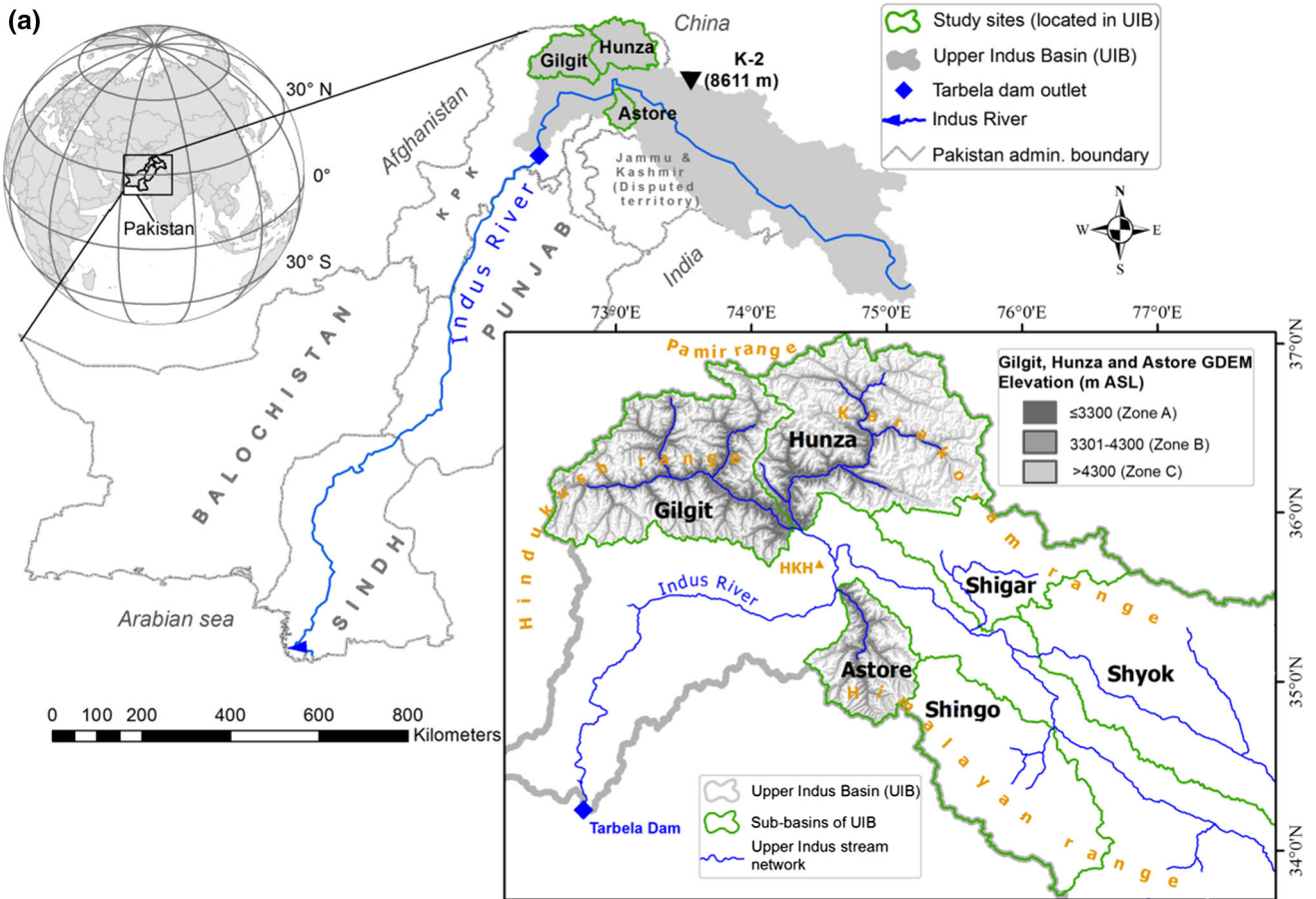
Springer

(a)

(b)

◄**Fig. 1 a** Map of Pakistan including the Upper Indus Basin (UIB) area, its sub-basins, the Tarbela dam and the Gilgit, Astore and Hunza sub-basin study sites, with their Global Digital Elevation Models GDEM, **b** mean monthly recorded precipitation totals (1951–2012) and mean monthly runoff (1980–2008) of the study sites. Precipitation records are the average totals of all the climate stations (Gilgit, Gupis, Ushkor and Yasin climate stations for the Gilgit basin; Astore, Rama and Rattu climate stations for the Astore basin; Khunjerab, Naltar and Ziarat climate stations for the Hunza basin) situated in the three catchments

irrigation water to the highly productive agricultural lands of the Pakistani Punjab (Fig. 1a) through a large network of barrages and canals (Indus Basin Irrigation System). Within the UIB, five river basins (Shyok, Shigar, Astore, Gilgit and Hunza) (Fig. 1a) contribute significantly to Indus River discharge. Principally fed by snow and glacier melt and little influenced by monsoon rainfall patterns because of the Western Himalayas mountain barrier, these five sub-catchments contribute nearly 70 % of the total Upper Indus flow (Mukhopadhyay and Khan 2014a) and thereby figure prominently in the management of the Tarbela reservoir. In addition, Liniger et al. (1998) estimated that over 80 % of Indus River flow reaching the plains originates in the Hindukush, Karakoram and Western Himalayan mountain areas.

As the UIB extends over parts of the Hindukush, Karakoram and Western Himalayan ranges, it is subjected to different micro climate regimes within the basin area. Most of the annual precipitation in the UIB (especially in the northern and western parts) occurs in the winter and spring and originates in the west (Dimri and Chevuturi 2014; Dimri et al. 2013; Young and Hewitt 1990). The effect of the monsoon decreases along the Himalaya–Karakoram–Hindukush Mountains moving from a south–east to north–west direction (Fowler and Archer 2005; Young and Hewitt 1990), making the climate of the northern and western parts of the UIB distinctly different from that of the eastern parts (Central Himalayas). There is a strong east–west gradient in monsoonal strength as it migrates along the Himalayan front (Bookhagen and Burbank 2006, 2010) such that the eastern parts of the UIB receive much more monsoon precipitation than the western parts. Two precipitation regimes influence the UIB discharge, i.e., (1) precipitation advected by westerly circulation, mainly in the form of snow at higher altitudes and winter rainfall at lower altitudes in the northwest (Hindukush–Karakoram region) and southwest (Western Himalayas) parts of the UIB (Dimri et al. 2013), and (2) the summer monsoon rainfall in the eastern part of UIB (Khan et al. 2015). Therefore, it is particularly important to investigate the hydro-climatological regime at the sub-basin scale to improve our understanding of the UIB's hydrology.

High elevation (>4000 m ASL) regions generate much of the UIB's flow (Archer 2003; Hewitt et al. 1989; Mukhopadhyay and Khan 2014a; Wake 1989; Young and Hewitt 1990). Despite this, only a few studies (e.g., Akhtar et al. 2008; Bookhagen and Burbank 2010; Immerzeel et al. 2012, 2015; Mukhopadhyay and Khan 2014a) have monitored the climatic parameters, snow and ice processes and resultant hydrological regimes at these altitudes. In remote regions, such as those of the UIB, satellite remote-sensing techniques may be the only way to analyze spatiotemporal variations in snow cover (Sirguey et al. 2009; Tahir et al. 2011). Moderate Resolution Imaging Spectroradiometer (MODIS) snow products have been widely used in estimating the spatial extent of snow cover in snowmelt runoff modeling applications (Immerzeel et al. 2009; Lee et al. 2005; Maurer et al. 2003). Several studies compared the relatively "coarse" resolution (500 m × 500 m) MODIS data, the "fine" resolution (30 m × 30 m) Advanced Spaceborne Thermal Emission and Reflection Radiometer (ASTER) data and ground observations in estimating snow cover; the former gave satisfactory estimates at both low and high altitudes (Tahir et al. 2011; Tekeli et al. 2005). The overall absolute accuracy of the 500 m resolution MODIS snow products is >90 % (Hall and Riggs 2007; Wang et al. 2008), but it varies by land-cover type and snow condition. These findings support the use of MODIS data in estimating changes in snow cover extent at varying altitudes and in different mountainous regions of the UIB.

The wide altitudinal range of the UIB (455 m ASL at Tarbela to 8611 m ASL at K2; Fig. 1a) and its resulting widely varying climate suggest that a global, basin-wide study regarding spatial variation in both snow cover and hydrological regime would not be as meaningful as a sub-basin scale study. To date, no studies have addressed these issues on the sub-basin scale of UIB, thus this study of individual UIB sub-basins situated in different mountainous regions under slightly different climate regimes (Fig. 1a) will contribute towards the improvement of water resources management for irrigated agricultural lands downstream of Tarbela. This study was different from previous studies on the UIB (e.g., Archer et al. 2010; Archer and Fowler 2004; Forsythe et al. 2012a, b; Fowler and Archer 2006; Hasson et al. 2014) in that the spatiotemporal trends of snow cover were estimated in three different altitudinal zones (contrary to the basin-wide-approach adopted previously) within a western sub-catchment of the UIB, the Gilgit sub-catchment in the Hindukush–Karakoram region. The trends and the hydroclimatic characteristics of the Gilgit sub-catchment were then compared to those obtained for a southern sub-catchment, Astore, in the Western Himalaya (Tahir et al. 2015; Fig. 1a) and a northern sub-catchment, Hunza, in the Central Karakoram region (Tahir et al. 2011; Fig. 1a). The

current study is an important complement to the two previous studies to better understand the water inputs of the Tarbela reservoir, and to provide a better representation of the climate diversity and dynamics and the land cover complexity.

The present study focused on (1) estimating annual and seasonal trends in hydro-meteorological variables e.g., snow cover extent, mean temperatures, precipitation and stream flow, (2) determining mutual correlations among the variables themselves, for the Gilgit River basin in the Hindukush–Karakoram range and (3) comparing the results to those previously obtained for the Astore and the Hunza River basins, which are also located within the greater UIB.

The Gilgit, Astore and Hunza River sub-catchments were selected for this study because they almost double the Upper Indus flow at their confluence with the Indus River. Hence, any change in their flow magnitudes or timing may strongly influence water resources management within the UIB. This study therefore contributes to a better understanding of the complex hydroclimatic regimes of the high-altitude snow- and glacier-fed river catchments typical of the UIB.

2 Study area

The snow- and glacier-fed Gilgit River basin (sub-basin of UIB) (Fig. 2) was selected for the analysis of snow cover extent and hydrological regime. These characteristics of the 12,656-km^2 Gilgit River basin were then compared to those of the previously studied 3990-km^2 Astore and 13,733-km^2 Hunza River basins (sub-basins of the UIB) (Fig. 1a) (Tahir et al. 2011, 2015). Snow and glacier melt water originating from two different ranges, Hindukush and Karakoram (Fig. 1a), feeds the Gilgit River basin. The Gilgit River originates in the Hindukush region, but the Karakoram glaciers also contribute significantly to its flow at the eastern boundary of the basin (Fig. 1a). While the climatic regimes of the Gilgit and Hunza River basins are almost similar, winter and spring in the Astore basin are much wetter (Fig. 1b). The Gilgit and Hunza River discharges are mainly dependent on the westerly circulation that promotes winter snowfall, and thereby generates high discharges under summer snow-melt conditions whereas the Astore River discharge is influenced by the winter and spring rainfall (at lower
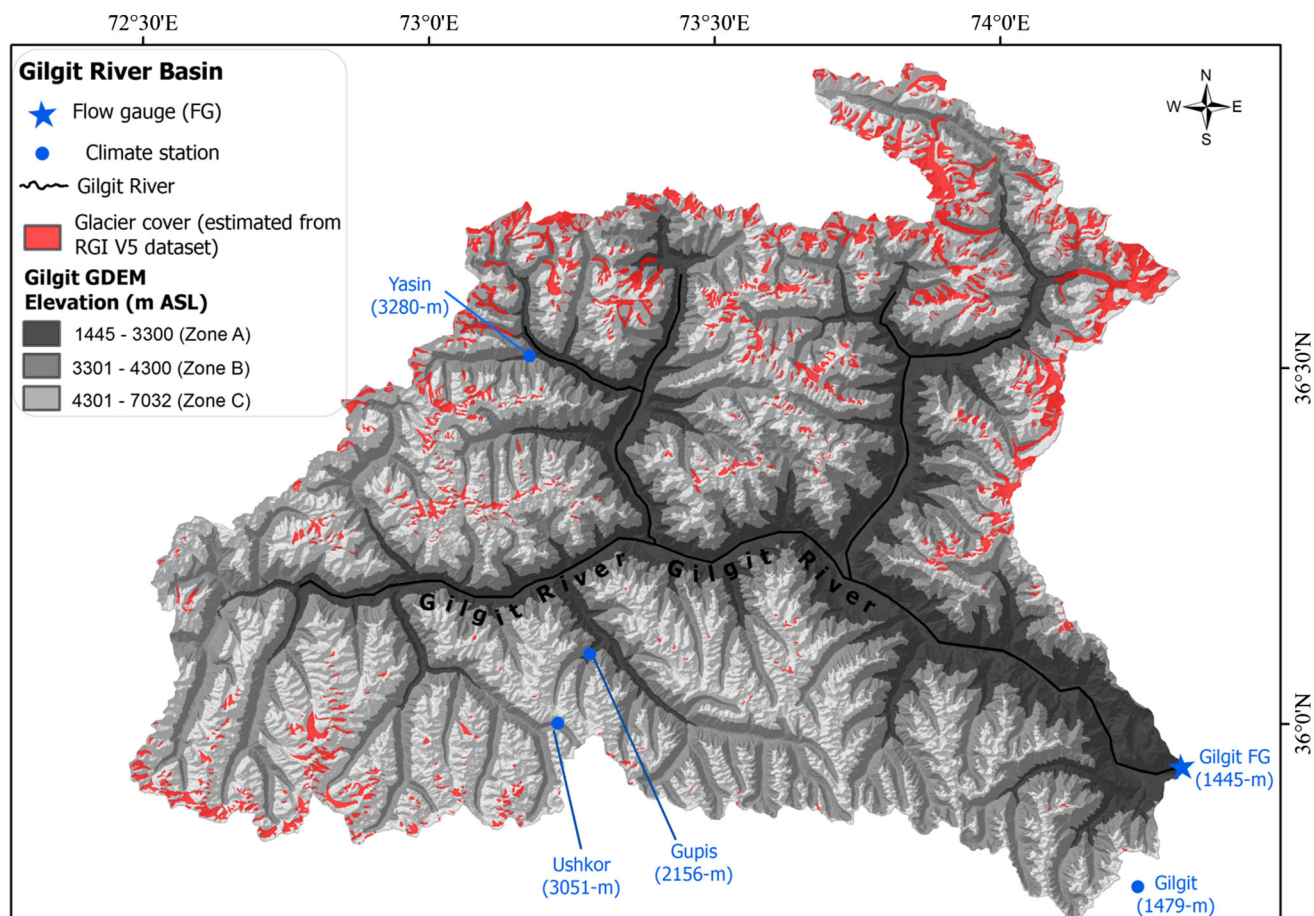

Fig. 2 Global Digital Elevation Model (GDEM) of the Gilgit River basin showing three altitudinal zones, glacier coverage across them, and superposed by the gauging stations

Table 1 Key features of the Gilgit, Astore and Hunza River basins

Catchment	Gilgit				Astore			Hunza		
River flow gauging station	Gilgit				Doyian			Dainyor bridge		
Latitude	35°56′N				35°33′N			35°56′N		
Longitude	74°18′E				74°42′E			74°23′E		
Elevation of gauging station (m ASL)	1445				1583			1450		
Drainage area (km^2)	12,656				3990			13,733		
Glacier-covered area (km^2)	∼1060				∼248			∼3417		
Glacier cover percentage (%)	∼8.37				∼6			∼25		
Mean elevation (computed from hypsometric curve) (m ASL)	∼4250				∼4100			∼4650		
Median elevation (computed from GDEM) (m ASL)	∼4150				∼4594			∼4631		
Area above 5000 m	(∼872 km^2) ∼ 7 %				(∼200 km^2) ∼ 5 %, (Tahir et al. 2015)			(∼4463 km^2) ∼ 32.5 %, (Tahir et al. 2011)		
No. of meteorological stations	4 (2 installed by PMD and 2 installed by WAPDA)				3 (1 installed by PMD and 2 installed by WAPDA)			3 (installed by WAPDA)		
	Gilgit 1479 m	Gupis 2156 m	Yasin 3280 m	Ushkor 3051 m	Astore 2168 m	Rama 3179 m	Rattu 2718 m	Khunjerab 4440 m	Ziarat 3020 m	Naltar 2898 m

Altitudes of the high-altitude climate stations were verified by the WAPDA (Water and Power Development Authority) and SIHP (Snow and Ice Hydrology Project) and corrected altitudes [different from those previously published by Archer (2003) and Tahir et al. (2011)] are given in the table

elevations), which combines with the solid winter precipitation forced by the Westerlies.

The main differentiating features of the Gilgit, Astore and Hunza River basins are summarized in Tables 1 and 2. The area of the Gilgit River basin was estimated using an ASTER Global Digital Elevation Model version-2 (ASTER-GDEM V2) at a 1 arcsec resolution (approx. 30 m). The hypsometric curve and the percentage area under each 500-m altitudinal layer, as estimated by the ASTER-GDEM V2 for the Gilgit, Astore and Hunza River basins, are presented in Fig. 3. The Gilgit, Astore and Hunza River basins differ most prominently in the relative areal distribution of their ≤3300, 3301–4300, and >4300 m altitudinal zones: 17, 39 and 44 %, respectively, for the Gilgit; 16, 50 and 34 %, for the Astore; and 11, 25 and 64 % for the Hunza River basin (Table 2). Only ≈5–7 % of the area in the Gilgit and Astore basins is above 5000 m ASL, while this percentage is ≈33 % in the Hunza basin (Fig. 3; Table 1). Mean elevations in the Gilgit, Astore and Hunza River basins are 4250, 4100 and 4650 m ASL, respectively, as determined from the hypsometric curve.

Three climate stations (Gupis, Yasin and Ushkor), equipped with precipitation gauges were installed at different altitudes within the Gilgit River basin and one station (Gilgit) just outside the catchment boundary (Fig. 2). Recorded average total annual precipitation (mean for the data period 1995–2008 for Ushkor and Yasin; 1951–2012 for Gupis and Gilgit) was 310, 313, 185 and 135 mm year^{-1} at the Ushkor (≈3051 m ASL), Yasin (≈3280 m ASL), Gupis (≈2156 m ASL) and Gilgit (≈1479 m ASL) climate stations, respectively. The Gilgit River's mean (taken over 29 years from 1980 to 2008) annual flow measured at the Gilgit hydrometric station (1445 m ASL; Fig. 2) was 285 ± 43 m^3 s^{-1}, resulting in an equivalent annual total water depth of 712 mm. The flow time series (m^3 s^{-1}) and the total catchment area (km^2) were inputted to the IRD (French Research Institute for Development) software HYDRACCESS developed by Vauchel (2005) to convert these flows into the equivalent water depths (mm).

Present precipitation records in the Gilgit basin are not representative of the runoff at the outlet because of the lack of climate data records at altitudes above ≈3300 m ASL and the underestimation of winter precipitation (snow). This may also be associated with well-identified high-mountain environment gauging errors (Førland et al. 1996; Sevruk 1985, 1989), including wind-induced error, wetting

Table 2 Main features of the elevation zones extracted from the ASTER GDEM of the Gilgit, Astore and Hunza River basins and their corresponding climate station

Zonal classification	Basin	Elevation band (m)	Mean elevation (m)	Median elevation (m)	Area (%)	Area (km²)	Climate stations
A (low-altitude zone)	Gilgit	1445–3300	∼2750	∼2372	17	2113	Gilgit, Gupis, Yasin, Ushkor
	Astore	1213–3300	∼2950	∼2263	16	638	Astore, Rama, Rattu
	Hunza	1432–3300	∼2850	∼2366	11	1541	Naltar, Ziarat
B (mid-altitude zone)	Gilgit	3301–4300	∼3900	∼3800	39	4915	–
	Astore	3301–4300	∼3910	∼3800	50	1995	–
	Hunza	3301–4300	∼3850	∼3800	25	3413	–
C (high-altitude zone)	Gilgit	4301–7032	∼4650	∼5578	44	5628	–
	Astore	4301–8069	∼4600	∼6132	34	1357	–
	Hunza	4301–7849	∼5000	∼6067	64	8779	Khunjerab

Elevation band area and mean elevation for each zone was computed from the hypsometric curve that was estimated from ASTER GDEM

loss, trace precipitation, blowing and drifting snow, and systematic mechanical errors. Another reason for this underestimation is that the spatially integrated precipitation value is largely influenced by orographic precipitation (a function of elevation and terrain characteristics) whereas the value recorded at a meteorological station is simply a point measurement.

3 Materials and methods

ASTER and MODIS products, ground observations of stream flow, climate data and their treatment for the Astore and Hunza River basins were explained in detail in two previously published studies by the authors Tahir et al. (2011, 2015). Similar datasets and methodologies were used for the Gilgit River basin to assess its spatiotemporal trends in snow cover and hydrological regime and then to compare the results to the Astore and Hunza River basins. A brief description of the data sets and methodology used for the Gilgit River basin is given below.

3.1 Topography

Based on ASTER image data available for high-latitude and steep mountainous areas (METI and NASA 2011), a GDEM V2 was used to sketch the river basin boundary. ASTER-GDEM V2 was preferred over Shuttle Radar Topography Mission (SRTM) because the former has a higher spatial resolution (∼30 m) than the latter (∼90 m). In addition, Nuimura et al. (2015) reported that ASTER-GDEM is a better product than SRTM to estimate the glacier covered area in high mountains. To allow a detailed analysis of spatial change in snow cover in the Gilgit, Astore and Hunza River basins, three altitudinal zones were extracted from the GDEM V2 for the study area

(Figs. 1a, 2; Table 2). These zones were based on the mean seasonal elevation of the freezing isotherms (0 °C). Using the studies of Hasson et al. (2014), Archer (2004) and Forsythe et al. (2012b), the zones were derived as follows: Zone A (≤3300 m) was the portion of the UIB below the winter (DJF) freezing isotherm ($T_{max} = 0$ °C), Zone C (>4300 m) included the portion of the UIB above the summer (JAS) freezing isotherm ($T_{min} = 0$ °C, as reported in Archer (2004) and Khan et al. (2015) this isotherm generally ranges between 5000–5500 m) and Zone B was the portion in between A and C. Total catchment and zonal areas, along with hypsometric curves and median elevations, were also estimated with the ASTER-GDEM V2 (Tables 1, 2; Fig. 3). The hypsometric curves were then used to calculate the mean elevations of the river basins and their respective altitudinal zones (Tables 1, 2).

The Randolph Glacier Inventory (RGI) Version 5 (V5) was used in this study to estimate the glacier cover over the Gilgit, Astore and Hunza River basins (Fig. 2; Table 1). RGI V5, released in July 2015, has new coverage of most of the Asian glaciers (Arendt et al. 2015) and is a combination of new and previously-published glacier outlines. Glacier outlines provided by Arendt et al. (2015) for the HKH region are entirely new in the current version and were taken from the GAMDAM Glacier Inventory (GGI) of Nuimura et al. (2015) and the second Chinese Glacier Inventory (CGI2) of Guo et al. (2015). For this reason the glacier cover estimated from RGI V5 for Gilgit, Astore and Hunza basins (Table 1) in this study differs from what was previously estimated from RGI V3.2 and presented by Tahir et al. (2015). RGI V5 is a globally complete inventory of glacier outlines and it is supplemental to the Global Land Ice Measurements from Space initiative (GLIMS). The RGI V5 offers complete one-time coverage, version control and a standard set of attributes (Arendt et al. 2015).
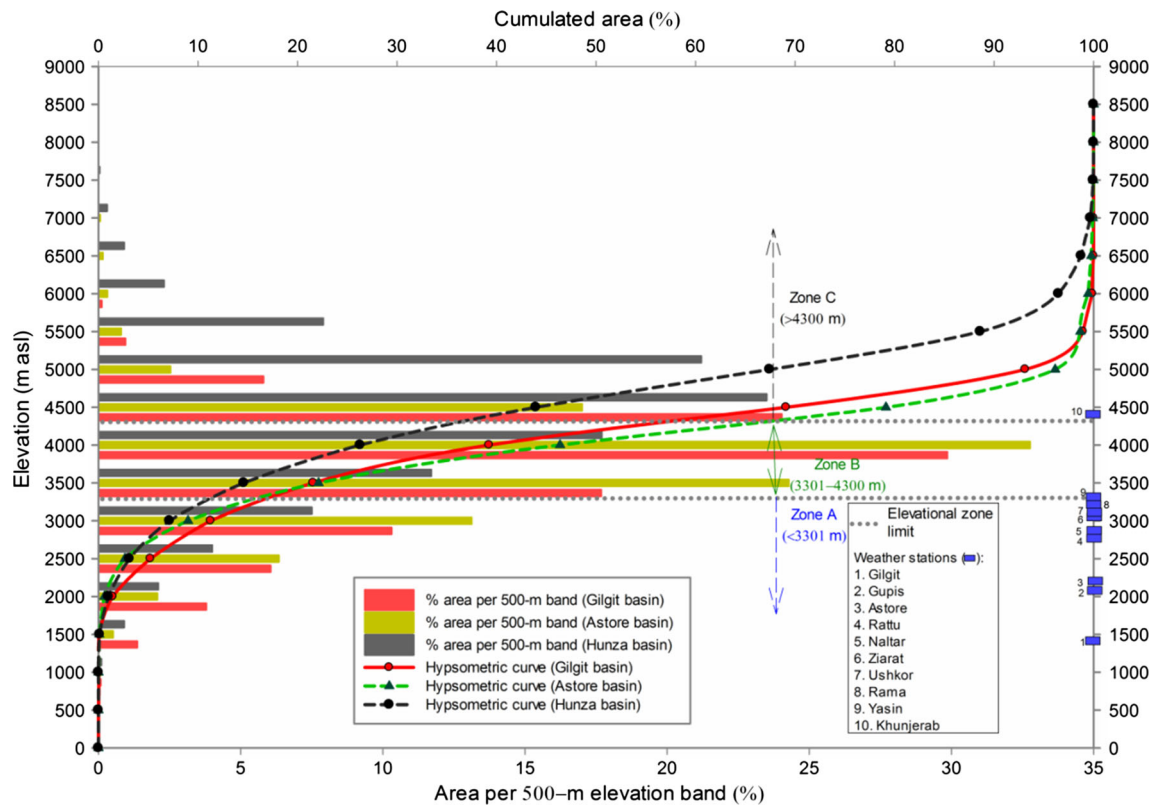
Fig. 3 Hypsometric curves, the distribution of area under 500-m elevation bands and the limits of elevation zones for the Gilgit, Astore and Hunza River basins, estimated from ASTER-GDEM V2. The location of the weather stations is presented on the *right hand side y-axis*

3.2 Hydrometeorology

The Surface Water Hydrology Project of the Water and Power Development Authority (SWHP–WAPDA) carries out the stream flow measurements in Pakistan, with the earliest observations dating from 1960. A 33-year database of daily discharge covering the period of 1970–2008 (with a missing data period for 1974–79) for the Gilgit River gauged at the Gilgit hydrometric station (Fig. 2) was available for this study. Meteorological data of daily mean temperatures and daily total precipitation over 14 years (1995–2008) for two high-altitude Automatic Weather Stations (AWS), Ushkor and Yasin (Fig. 2), was provided by the WAPDA, and similar data over a ∼62 year time period (1951–2012) from two valley stations, Gilgit and Gupis (Fig. 2), was provided by the PMD (Pakistan Meteorological Department).

The nonparametric Mann–Kendall (MK) trend test for periodic data, with a 5 % significance level ($P = 0.05$) for Kendall's tau (τ) coefficient (Hirsch and Slack 1984; Hirsch et al. 1982; Kendall 1975; Mann 1945; Mukhopadhyay and Khan 2014b; Pellicciotti et al. 2010; Nalley et al. 2012; Pingale et al. 2014), and the Theil–Sen estimator or "Sen's slope" S (Gilbert 1987; Sen 1968) were applied to identify trends in the time series data. The MK trend test is a nonparametric test that is less sensitive to

extreme sample values and is independent from the hypotheses regarding the nature of either linear or nonlinear trends (Nalley et al. 2013; Araghi et al. 2015). Sen's slope is a method for robust linear regression that chooses the median slope among all lines through pairs of two-dimensional sample points. A seasonal trend analysis of the precipitation and temperature data was performed for the winter months from December to February (DJF) and the summer months from July to September (JAS) on 62 years of climate data (1951–2012) of the Gilgit and Gupis climate stations. Trends on the standardized values (as per the standardization procedure outlined by Tahir et al. 2015) of annual runoff (for the Gilgit, Astore and Hunza rivers) and total annual precipitation (recorded at the Gilgit climate station) were also calculated.

An analysis of the annual and seasonal (winter and summer) relationships between different variables (precipitation, snow cover, mean temperature and discharge) were also carried out using different correlation tests (explained in Tahir et al. 2015) at a 5 % significance level.

3.3 Snow cover

The MODIS/Terra Snow Cover 8-Day L3 Global 500-m Grid (MOD10A2) dataset over the period of March 2000–

December 2012 was used to estimate the snow cover extent; it contains fields for maximum snow cover extent over an 8-day period (Hall et al. 2006, updated weekly) at a resolution of approximately 500 m (precisely, 15 arcsec) and completely covers the Gilgit River basin. The Gilgit River basin area was then extracted from larger tiles (h23–v05 and h24–v05 tiles; "*h*" denotes horizontal and "*v*" denotes vertical) to estimate the spatial extent of snow cover (%) for the different elevation bands/zones (Table 2) over the 13-year period. A limitation of the MOD10A2 is that persistent cloud cover over consecutive days or over all days of the 8-day period can hide snow cover that might have existed (Hall and Riggs 2007). The uncertainties of this product [caused mainly by the confusion between the snow and cloud signals or by the use of the maximum snow covered area (SCA) over the 8-day period] are not currently well known in high altitude areas (Hall and Riggs 2007). The daily MODIS snow product (MOD10A1) was not utilized in this study because of the significant gaps in the times series, especially during the monsoon season, as a result of cloud cover (Savéan et al. 2015), and also because of the low quality of this product in the HKH area (Ragettli et al. 2015). MODIS snow products (MOD10A2) used in the current study were treated to avoid the inaccuracies in snow cover estimation due to cloud cover following the procedure detailed by Tahir et al. (2015). The entire data series was also subjected to a seasonal climatology adjustment (Mukhopadhyay and Khan 2014b; Pellicciotti et al. 2010) before trend analysis. Seasonality is a pattern in a time series that replicates systematically, in this case every year. Seasonal fluctuations make it difficult to analyze the trend in data for a given period because of confusion as to whether the change reflects an ample change in the magnitude of the data or is due to regularly occurring seasonal variation. Seasonal adjustment (de-seasonality) was applied to assess the seasonal variation and to omit its impact on a time series; the result was a seasonally adjusted (de-seasonalized) time series. Trends in the snow cover time series were then determined using Kendall's tau (τ) and Sen's slope (*S*) at a significance level of 5 %.

4 Results and discussion

4.1 Changes in snow cover in the Gilgit River basin

In the Gilgit River basin, the 13-year annual mean extent of snow cover, estimated from MODIS snow products, varied between ≈ 85 % (in winter) and ≈ 12 % (in summer) (Fig. 4). Snow began to accumulate in September and peak snow cover (~ 85 %) generally occurred in late January to mid-February (Fig. 4). Generally, July to September are the months of glacier melt flow from the area

(Mukhopadhyay and Khan 2015), so the appearance of snow accumulation starting in September (Fig. 4) might have been associated with snow accumulation at higher altitudes. Spring snowmelt began in early April (Fig. 4) resulting in an increase in river discharge (Fig. 1b) and the minimum snow cover (~ 12 %) was reached in August. Approximately 872-km^2 of the Gilgit River basin's area exists at elevations exceeding 5000 m ASL (see hypsometric curve, Fig. 3), with almost the same area (≈ 8 %) being glaciated. This information was extracted from the GDEM V2 of the Gilgit River basin (Fig. 2) using the RGI (Randolph Glacier Inventory) version 5 dataset (Arendt et al. 2015) as a mask. The average snow cover cycle in the Gilgit, Astore and Hunza River basins over the entire study period are shown by a solid and two dashed lines, respectively, in Fig. 4.

Trends in monthly snow cover were estimated for a 13-year period in three altitudinal zones (low, 1450–3300 m; mid, 3301–4300 m; and high elevation zone, 4301–7032 m) of the Gilgit River basin (Fig. 5). In the low altitude zone, the MK trend analysis showed a significant positive trend in snow cover (Fig. 5) over the 13-year data period. In contrast, for the middle and high altitude zones the positive trend was non-significant. For the low, mid and high elevation zones the τ values were +0.26, +0.124 and +0.079, respectively, while S values (% year^{-1}) were +0.021, +0.018 and +0.024, respectively (Fig. 5).

In the middle and high elevation zones, covering ~ 39 and ~ 44 % of the total Gilgit basin, respectively, snow is the main form of precipitation. In contrast, the low elevation zone, which covers ~ 17 % of the Gilgit basin's total area, receives most of its precipitation in the form of rainfall and houses the outlet of most of the region's glaciers (Fig. 2) to streams and rivers. This zone may prove more sensitive to the overall variation in basin snow cover extent since it has the largest proportion of glacier-free area among the three zones and it experiences the highest temperatures. For these reasons, it is most vulnerable to changes in precipitation from snow to rainfall due to a warming climate. The lower elevation zone is also the portion of the basin area where positive trends in snow cover extent were strongest ($\tau = +0.26$, $P < 0.05$; $S = +0.021$ % year^{-1}) and may therefore greatly influence the overall trends in basin snow cover. Moreover, the high elevation zone of the Gilgit River basin is largely covered by glaciers, particularly at elevations exceeding 5000 m ASL (Fig. 2; Table 2) and thus the detection of changes in snow cover (especially wet snow) is difficult owing to the similar spectral properties (Gupta et al. 2005).

In comparison, positive trends in snow cover extent were found in the Astore River basin (Tahir et al. 2015) and stable trends were found in the Hunza River basin
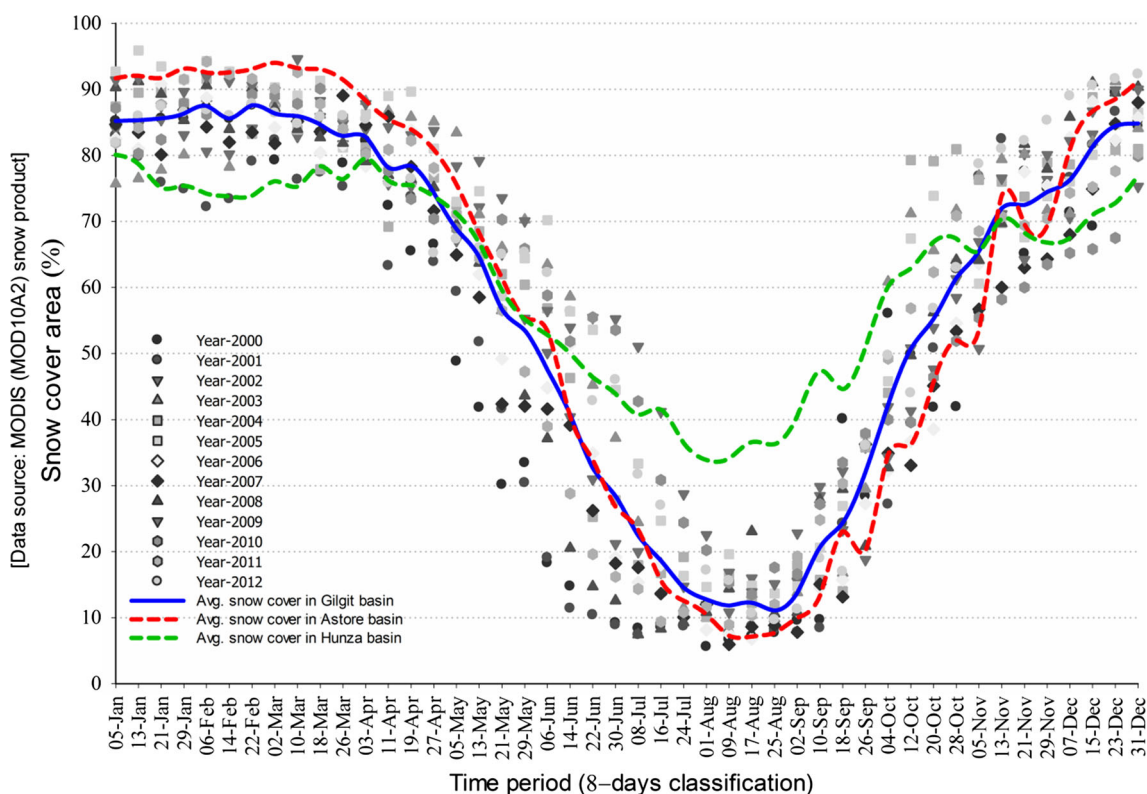
Fig. 4 Annual cycle in snow covered area as a percentage of total area estimated through the analysis of 600 MODIS snow images (*scatter plot*) for 13 individual years (2000–2012) in the Gilgit River basin and average snow cover area *curves* for the Gilgit, Astore and Hunza basins

(Tahir et al. 2011). In Astore, tau (τ) coefficient values were significant ($P < 0.05$) with +0.066, +0.088 and +0.058 for the zones A, B and C, respectively, and in the Hunza River basin these values were non-significant with +0.01, −0.01, +0.03, respectively. In the mid-elevation zone, trends were positive but non-significant for both the Gilgit ($\tau = +0.124$), and the Hunza ($\tau = -0.01$) River basins (Fig. 5; Tahir et al. 2011). This value did not have a significant effect on the overall trend in snow cover extent in the Hunza River basin since nearly 75 % of the Hunza catchment area was not within this elevation zone (Fig. 3; Table 2). In contrast, for the Astore basin, the snow cover trend was significant ($\tau = +0.088$; $S = +0.270$ % year^{-1}) in the mid-elevation zone. This zone contains almost 50 % of the Astore catchment area and hence significantly influences its overall snow cover extent. In the low elevation zone, where a significant positive trend in the extent of snow cover existed in the Gilgit and Astore River basins but not in the Hunza River basin, the snow cover trend effect would again be minor given that only 17 and 16 % of the area of the Gilgit and Astore basins, respectively, is in the lower elevation zone. The essentially constant snow cover extent of the other Gilgit River basin zones was a key factor in the overall unchanging or statistically non-significant increasing snow covered area in the catchment.

While analyzing the basin-wide trends, snow cover extent was stable in the Gilgit, Astore and Hunza River basins: $\tau = +0.33$, $\tau = +0.03$ and $\tau = +0.02$, respectively (Table 3). Mean snow cover values referring to snow accumulation (DJF) and snowmelt (JAS) seasons were calculated for each year and the MK trend test was applied to these annual mean values. In the Gilgit River basin, a slightly increasing but non-significant trend in snow cover extent was observed in both the snow accumulation and the snowmelt periods ($\tau = +0.23$, +0.26, respectively; Table 3), whereas for the Astore and Hunza River basins, a significant increasing trend occurred during the snow accumulation period ($\tau = +0.06$ and $\tau = +0.25$, respectively). During the snow melt period, only the Astore basin registered a significant increase in snow cover ($\tau = +0.07$) while the Hunza basin showed almost constant snow cover extent ($\tau = +0.01$). The trend analysis of mean temperature and total precipitation over the same period is presented in Fig. 5, and may help determine the factors behind this consistent snow cover trend. A Kendall tau coefficient value of $\tau = +0.15$ for precipitation and $\tau = -0.21$ for the mean temperature trend was determined over the 13-year period (2000–2012) (Fig. 5). This increasing trend of precipitation and decreasing trend of mean temperatures over the

Fig. 5 Gilgit River basin: Linear trend analysis of total recorded precipitation and mean temperature (average of Gupis and Gilgit climate stations for the period 2000–2012, *top panel*). Trend of MODIS-data-derived snow covered area (seasonally adjusted time series) in three altitudinal zones over the same 13-year period 2000–2012 (*bottom three panels*). Trend was analyzed using the linear trend line equation, Mann–Kendall's trend test "τ" and Sen's slope estimator "S"
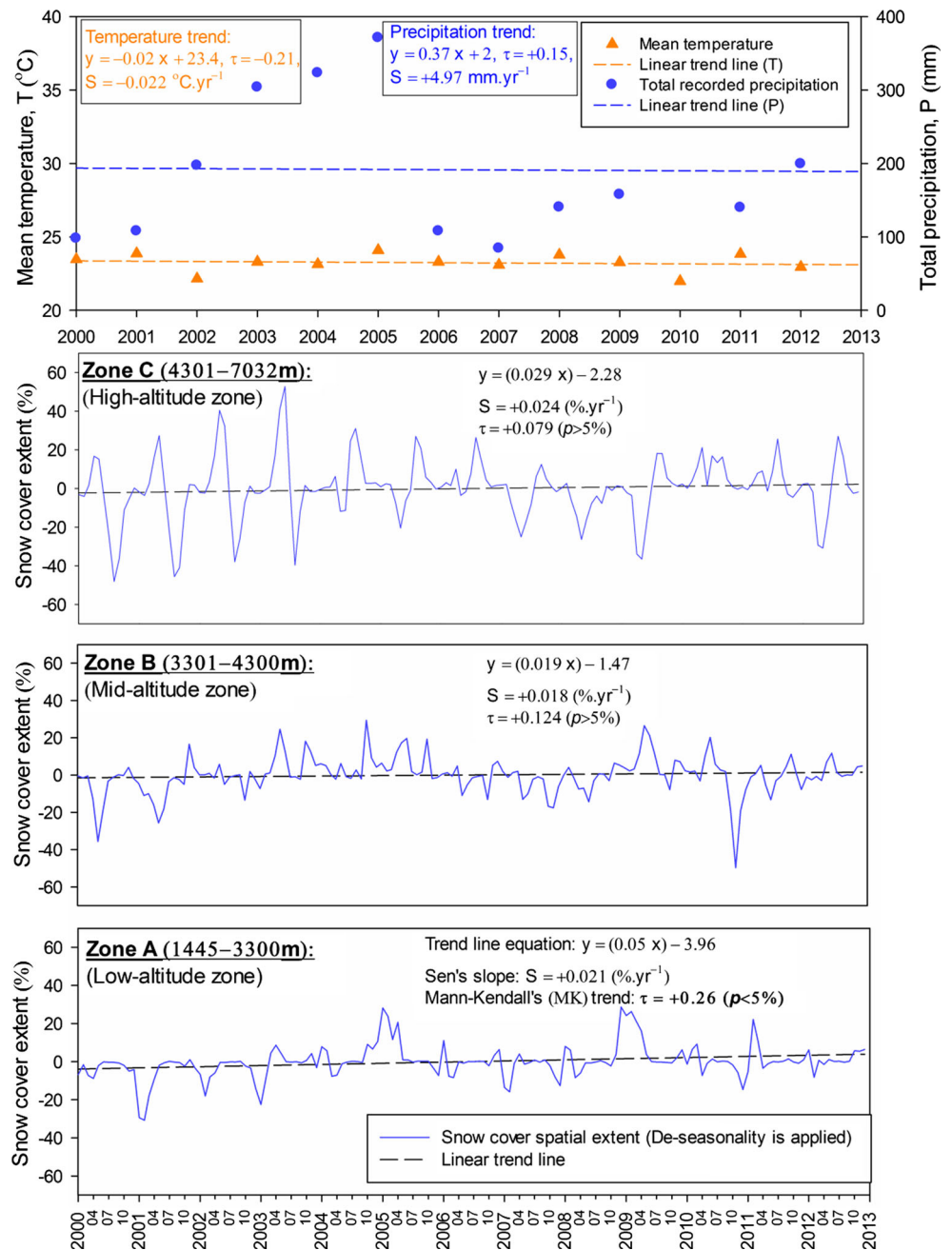
same period (2000–2012) indicated the possible reasons for the stable trend in snow cover. The increasing trends of precipitation continued to feed the high altitudes and the decreasing trend of mean temperature reduced the snowmelt losses and resulted in stable or slightly expanding snow cover, which was very similar to the Astore and Hunza River basins.

Long term (1951–2012) seasonal trends in mean temperature and total recorded precipitation (Fig. 6) might help determine which climatic factors have led to the stable or very slight, non-significant increasing snow cover

extent seen in these three river basins. For the Gilgit River basin, over the 62-year period (1951–2012), trends in total winter and summer recorded precipitation were positive ($\tau = +0.10, +0.07$, respectively) but non-significant, as was the downward trend in mean winter temperature ($\tau = +0.123$; Fig. 6). Only the downward trend in mean summer temperature ($\tau = -0.21$) was significant (Fig. 6), which provided a possible reason for the stable trend in snow cover extent. In a manner similar to the Astore and Hunza River basins (Tahir et al. 2011, 2015), decreasing trends in mean summer temperature reduced snow losses

Table 3 Analysis of spatiotemporal change (basin wide, BW) in snow covered area (SCA), hydrological regime (runoff Q) and climatic parameters (precipitation P, mean temperature T_{avg}) for the Gilgit (current study), Astore and Hunza (previous studies) River basins

	Gilgit River basin	Astore River basin	Hunza River basin
Basin wide SCA annual range (%)	12–85	7–95	30–80
BW SCA (monthly) trend (2000–2012)	$\tau = +0.33$	$\boldsymbol{\tau = +0.03}$	$\boldsymbol{\tau = +0.02}$
BW SCA DJF trend (2000–2012)	$\tau = +0.23$	$\boldsymbol{\tau = +0.06}$	$\boldsymbol{\tau = +0.25}$
BW SCA JAS trend (2000–2012)	$\tau = +0.26$	$\boldsymbol{\tau = +0.07}$	$\tau = +0.01$
Hydrological regime			
Mean annual runoff	712-mm (data period, 1980–2008)	1084-mm (data period, 1974–2007)	759-mm (data period, 1966–2008)
Total annual recorded P	135-mm at Gilgit	501-mm at Astore	680-mm at Naltar
	185-mm at Gupis	723-mm at Rattu	225-mm at Ziarat
	310-mm at Ushkor	794-mm at Rama	170-mm at Khunjerab
	313-mm at Yasin		
Correlations (annual)			
Q vs SCA change	**−0.86**	**−0.56**	**−0.89**
Q vs T_{avg}	**+0.84**	**+0.75**	**+0.85**
Q vs P	**+0.19**	**−0.28**	**+0.08**
SCA change vs T_{avg}	**−0.87**	**−0.89**	**−0.80**
Correlations (seasonal)			
DJF P vs DJF SCA	+0.14	**+0.44**	+0.01
JAS Q vs DJF P	+0.48	**+0.76**	+0.1
JAS Q vs JAS T_{avg}	**+0.65**	**+0.52**	**+0.81**
Annual Q vs JAS P	−0.30	+0.19	+0.005
Trend analysis: runoff Q	Increasing trend	Increasing trend	Decreasing trend
Seasonal P	Increasing trend	Increasing trend	Increasing trend
JAS T_{avg}	Decreasing trend	Decreasing trend	Constancy
SCA	Constancy/slight increase	Constancy/slight increase	Constancy/slight increase

Trends are expressed using the Kendall's tau coefficient and significant ($P \leq 0.05$) trends/correlations are indicated in bold

*DJF* December–January–February, *JAS* July–August–September

from high altitudes and resulted in stable or slightly but not significantly expanding snow cover.

The current hypothesis for this phenomenon of stable or slightly increasing snow cover is an increase in winter precipitation (snow-depth) (though not significant in this study) and a decrease in the mean summer temperature as presented in Fig. 6 and explained by Hewitt (2005) and Archer and Fowler (2004). This increased amount of snow at lower altitudes might not have melted away by the end of the spring season and hence caused the snow covered area to increase at these lower altitudes (Fig. 5). Increasing trends of annual and seasonal precipitation in the Asian region were also confirmed by the IPCC's 5th synthesis report (Hartmann et al. 2013). Ridley et al. (2013) assessed the changes in the severity and frequency of snowfall events due to weather patterns, such as the Westerlies, using a regional climate model and indicated an increase in the frequency of occurrence up to the end of 21st century.

They explained that the Karakoram glaciers may continue to grow, or decline at a slower rate, compared with those across the rest of the Himalayas due to this increase in snowfall events. Treydte et al. (2006) provided a millennial-scale reconstruction of precipitation change through an annually resolved oxygen isotope record from tree-rings in the high mountains of northern Pakistan and an increase in the precipitation during the late 19th and the 20th centuries was found that yielded the wettest conditions of the past 1000 years. These climate change trends in the UIB play an important role in stabilizing or minimally expanding snow cover, especially in the North–West Hindukush, Central Karakoram and Western Himalaya regions of Pakistan. A constant or marginally increasing trend in snow cover extent in the Gilgit, Astore and Hunza River basins, situated in different mountain ranges, indicated that the trend may be similar in the rest of the Upper Indus River catchment, but this needs to be verified.

Fig. 6 Trend analysis for climate parameters monitored at Gilgit and Gupis meteorological stations **a** total summer (JAS) and winter (DJF) recorded precipitation and **b** mean summer (JAS) and winter (DJF) temperature, over the period 1951–2012

Trend analysis	(a) Total recorded precipitation		(b) Mean temperature	
	Summer (JAS)	Winter (DJF)	Summer (JAS)	Winter (DJF)
Linear equation	y=0.25x + 30.8	y=0.14x + 12. 2	**y=- 0.02x + 25.8**	y=0.01x + 5
MK, τ	+0.10 ($p>0.05$)	+0.07 ($p>0.05$)	**- 0.21 ($p<0.05$)**	+0.12 ($p>0.05$)
Sen's slope, S	+0.17 (mm.yr^{-1})	+0.075 (mm.yr^{-1})	**- 0.02 (°C.yr^{-1})**	+0.01 (°C.yr^{-1})
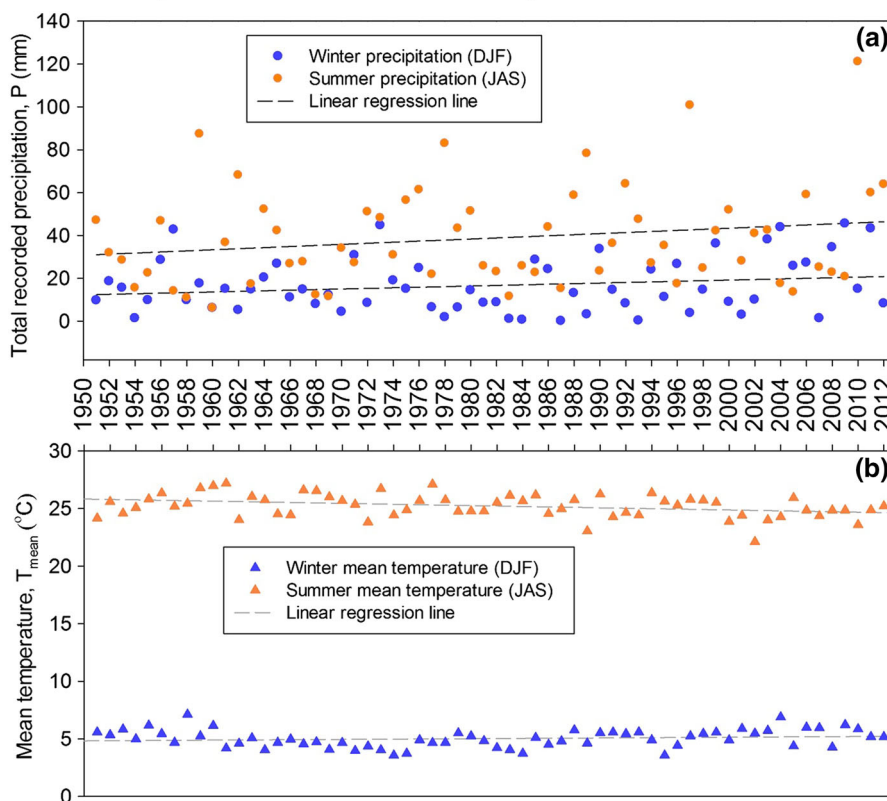
4.2 Trend analysis of stream flow, winter and summer total precipitation and mean temperature in the Gilgit River basin compared with the Astore and Hunza River basins

Trend analysis of the standardized values of annual runoff measured at the Gilgit hydrometric station in the Gilgit River basin is presented in Fig. 7. A non-significant trend of increasing discharge was found for the Gilgit River over 29 years of flow records (1980–2008); $\tau = +0.207$ and the Sen's slope value was $+3.3$ mm year^{-1} (Fig. 7). Immerzeel et al. (2013) and Mukhopadhyay and Khan (2014b) reported the same rising trend in runoff from the glacierized river basins of Himalaya and Karakoram, respectively.

The flow trend for the Gilgit River basin was similar to the Astore basin but contrasted with the flow trend for the Hunza River where stream flow has been decreasing non-significantly (Fig. 7), possibly as a result of cooling temperatures at

higher altitudes, which decelerate snow and glacier melt, especially in summer. The snow cover in the Gilgit catchment showed a stable or slightly rising trend (although not significant at mid- and high altitude zones; Fig. 5), thus the trend toward increasing but non-significant annual discharge in the Gilgit River can be related to the trend of increasing summer precipitation as analyzed in this study (Fig. 6) and reported by the IPCC's 5th synthesis report (Hartmann et al. 2013) and Archer and Fowler (2004).

Climate variables (seasonal precipitation and mean temperature) that have an effect on Gilgit River discharge and snow cover were analyzed to confirm the trends reported by (1) Ridley et al. (2013) in the regional climate modeling study, (2) Archer and Fowler (2004) in the precipitation study over the 1895–1999 period and (3) Archer (2003) in the hydrological regime study over the 1900–1999 period, for the UIB, including the Gilgit climate station. An analysis of the (1) total recorded seasonal
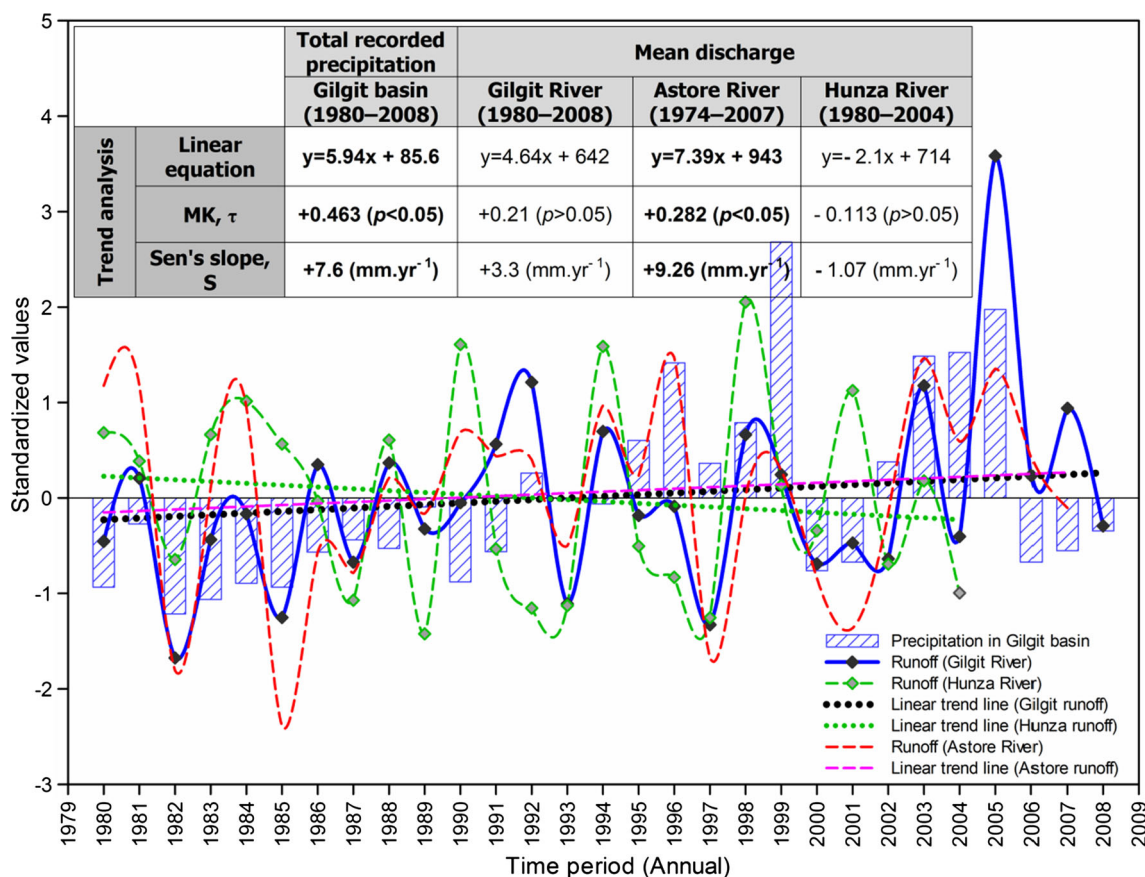
Trend analysis		Total recorded precipitation	Mean discharge		
		Gilgit basin (1980–2008)	Gilgit River (1980–2008)	Astore River (1974–2007)	Hunza River (1980–2004)
	Linear equation	y=5.94x + 85.6	y=4.64x + 642	y=7.39x + 943	y=- 2.1x + 714
	MK, τ	+0.463 ($p<0.05$)	+0.21 ($p>0.05$)	+0.282 ($p<0.05$)	- 0.113 ($p>0.05$)
	Sen's slope, S	+7.6 (mm.yr^{-1})	+3.3 (mm.yr^{-1})	+9.26 (mm.yr^{-1})	- 1.07 (mm.yr^{-1})

Fig. 7 Trend in standardized values of annual flow in the Gilgit River (monitored at the Gilgit hydrometric station), Astore River (monitored at Doyian) and Hunza River (monitored at the Dainyor hydrometric station), and total annual recorded precipitation (mean of Gilgit and Gupis meteorological stations) over 29 years (1980–2008)

precipitation (mean of Gilgit and Gupis climate stations) and (2) mean seasonal temperature (mean of Gilgit and Gupis climate stations) for a 62-year time series (1951–2012) was performed for the winter (DJF) and summer (JAF) periods in the Gilgit River basin (Fig. 6). Trends for the total recorded seasonal (winter and summer) precipitation and the mean winter temperature were not significant, even though they presented a slight increase and decrease, respectively (Fig. 6). A significant decreasing trend ($\tau = -0.21$, $S = -0.02$ °C year^{-1}) was found for the mean summer temperature. An increase in total recorded precipitation was found during summer and winter seasons with a Sen's slope value of +0.17 and +0.075 mm year^{-1} ($\tau = +0.10$ and +0.07; $P > 0.05$), respectively. These results were in accordance with the findings of Ridley et al. (2013), Archer and Fowler (2004) and Archer (2003), who found a less significant trend (lower τ values at a 5 % significance level) than in the present analysis. Mean winter temperature showed a non-significant increasing trend ($\tau = +0.123$) with a Sen's slope value of +0.01 °C year^{-1}. Even if this trend was positive, the mean winter temperature still remained negative in high-altitude zones of snow

accumulation. The effect of the positive trend can become important if the temperature continues to rise at the same rate over the next few years.

4.3 Correlation between snow cover, climate variables and stream flow in the Gilgit River basin (hydrological behavior) and comparison to the Astore and Hunza basins

The relationships existing between standardized values of precipitation, snow cover, mean temperature and discharge of the Gilgit River basin are presented in Fig. 8. The snow cover extent showed a significant inverse correlation with the mean temperature and water discharge in the Gilgit River basin. In fact, high temperatures increased snow melt which in turn resulted in reduced snow cover and increased river discharge. Conversely, low temperatures resulted in longer snow cover duration and reduced river discharge. The discharge reached its peak from July to September (Fig. 8) in the Gilgit River as a result of increasing snow and glacier melt. It is likely that the substantial snow cover variability (difference between consecutive months) has a
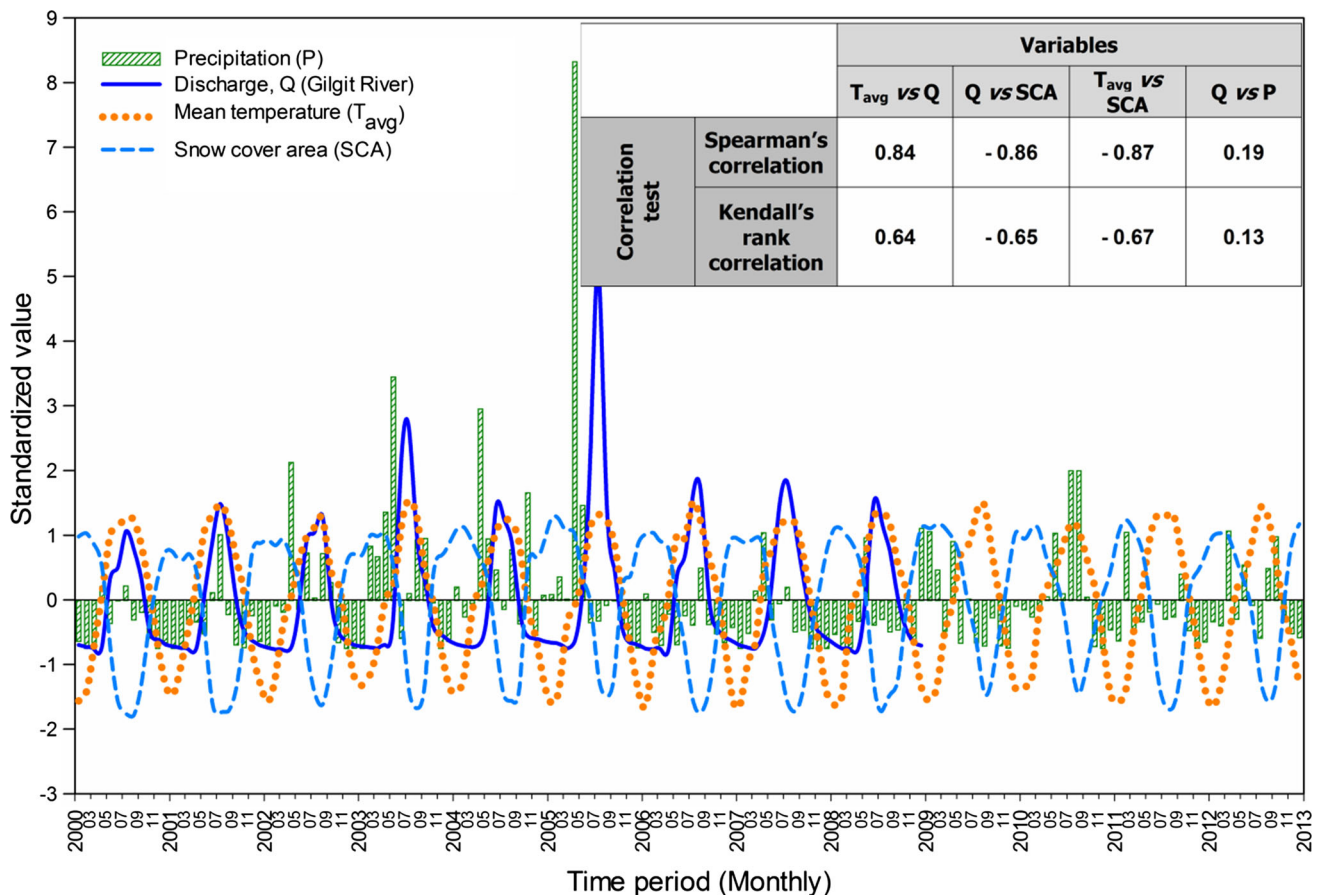
Fig. 8 Gilgit River basin: correlations between standardized values of monthly precipitation, snow cover extent, mean temperature and discharge. Significant ($P \leq 0.05$) correlations are indicated in *bold*

large impact on discharge because a larger snow covered area may also result in greater snow depths (at least in low-slope valley areas).

On an annual basis, we did not find a significant correlation ($r = +0.14$; $P > 0.05$) between winter snow cover extent and winter precipitation in the Gilgit River basin (Table 3). A possible explaination of the non significant correlation can be that the actual amount of winter precipitation was unknown due to previously explained gauging errors and a lack of climate stations at high altitudes. A positive correlation (though not significant) was found between the winter precipitation and summer discharge ($r = +0.48$) (Table 3), which indicated that the accumulation of snow during winter generates discharge upon snow melting in the summer season. As expected, the summer discharge was significantly correlated ($r = +0.65$) with the summer mean temperatures in the catchment area, indicating that the seasonal discharge in the Gilgit River is driven by temperature seasonality of flow arising from the melting of the snow and glaciers of the Gilgit River basin.

A correlation between the monthly difference (difference between consecutive months) in discharge and in the snow covered area for the Gilgit, Astore and Hunza River basins is presented in Fig. 9. The two variables were inversely and significantly correlated for these three river catchments (Fig. 9), which indicated that the change in river discharge is dependent largely on the snow cover change in these catchment areas; a decrease in snow cover generally corresponded to an increase in the discharge and vice versa. For the Gilgit River basin, the Pearson product moment correlation (Rodgers and Nicewander 1988), Spearman rank order correlation (Spearman 1904) and Kendall's rank correlation (Kendall 1975; Kendall and Gibbons 1990) values were -0.57, -0.76, and -0.59, respectively. These values were -0.73, -0.75 and -0.56, respectively, (Fig. 9) for the Hunza River basin and the Astore basin had correlation values of $r = -0.39$ (Pearson's correlation coefficient), $r = -0.48$ (Spearman's rank correlation) and $r = -0.36$ (Kendall's rank correlation), which was much lower in absolute value than those for the Gilgit and Hunza River basins (Fig. 9) owing to its lower mean elevation and the higher influence of summer precipitation on discharge (Table 3).
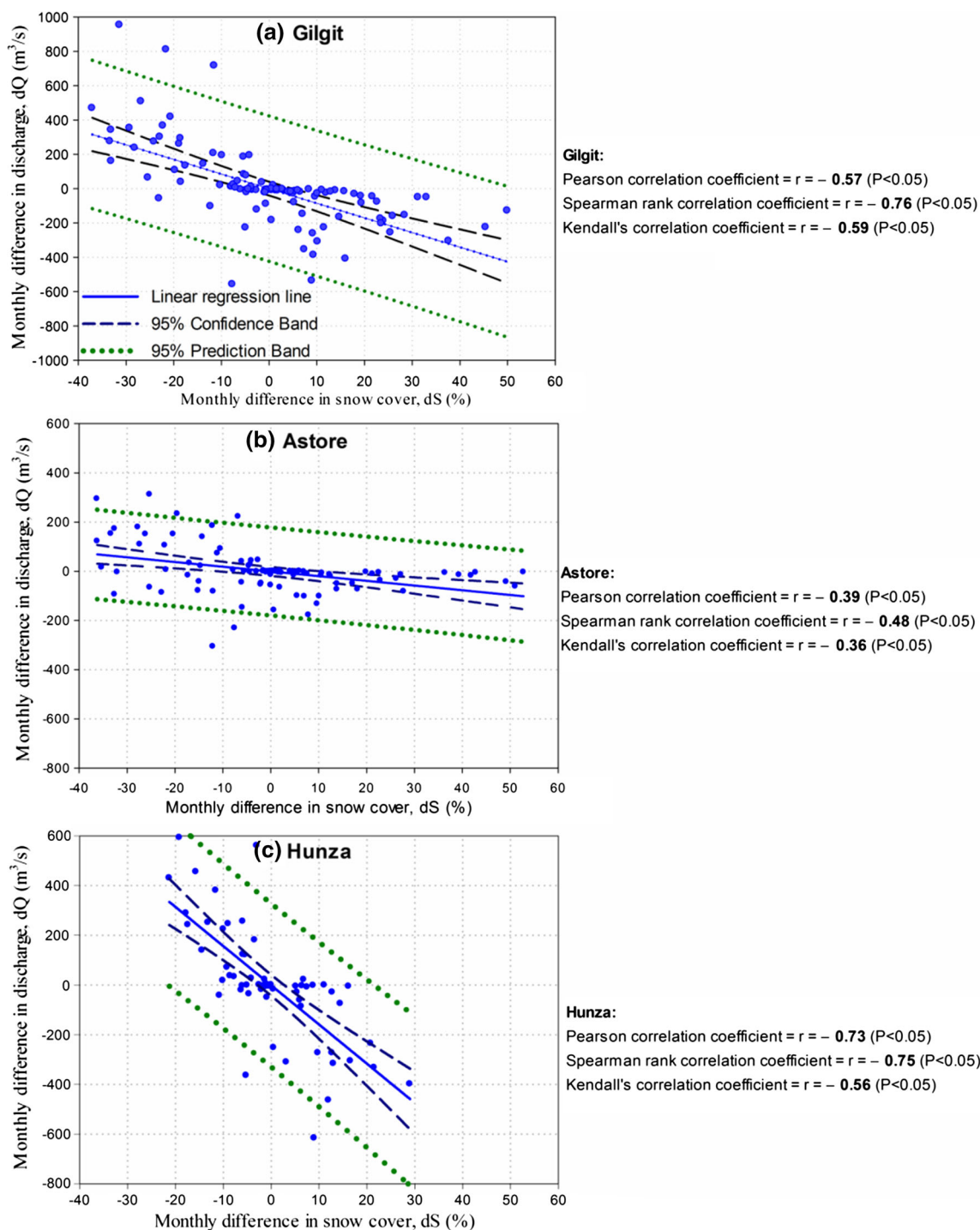
Fig. 9 Correlation between monthly difference (difference between two consecutive months) in snow cover and monthly difference in discharge in the **a** Gilgit, **b** Astore and **c** Hunza River basins. All correlation coefficients are significant ($P \leq 0.05$)

5 Discussion and comparison of the physical and hydrological characteristics of the Gilgit, Astore and Hunza River basins

Table 3 presents a summary of the snow cover trends, the hydrological regimes and the correlation between different hydro-meteorological variables (stream flow, snow cover extent, temperature and precipitation) in the three catchment areas (Gilgit, Astore and Hunza). The Gilgit basin is a mid-altitude (mean elevation ≈ 4250 m) snow- and glacier-fed catchment (mean annual runoff ≈ 712 mm) situated in the Hindukush–Karakoram ranges, with a small percentage of glacier cover (≈ 8.37 %). The Hunza River basin is a comparatively higher-altitude (mean elevation

≈ 4650 m) snow- and glacier-fed catchment (mean annual runoff ≈ 759 mm) situated in the Central Karakoram region with a large concentration of glaciers (≈ 25 % glacier cover). Both catchments are dependent on temperature seasonality for the generation of runoff in the spring and summer seasons. The Astore River basin, on the other hand, is a comparatively lower-altitude (mean elevation = 4100 m ASL) high-runoff (mean annual runoff = 1084 mm) catchment situated in the Western Himalayas in the south of Karakoram that had a good correlation between the summer stream flow and the current summer and preceding winter precipitation amounts.

5.1 Snow cover change

The Gilgit and Astore River basins had a greater annual range of variability in snow cover (85–12 % and 95–7 %, respectively; Fig. 4) than the Hunza River basin, which may be attributed to differences in the mean elevation (4250 and 4100 m ASL, respectively) and glacier cover (≈ 8.37 and ≈ 6 %, respectively) of the Gilgit and Astore River basins compared to the Hunza River basin (mean elevation = 4650 m ASL and glacier cover = ∼ 25 %). The Gilgit and Astore River basins only have ≈ 5–7 % of their area above 5000 m ASL (Fig. 3; Table 1), compared to the Hunza River basin, which has ≈ 33 % of its area above this altitude (Fig. 3; Tahir et al. 2011). An increase in mean temperature in a small area at a lower altitude (such as in the Astore River basin) results in more rapid snow cover depletion than in a larger area at a higher altitude (Tahir et al. 2015). Similarly, a snowfall event can cover the smaller area more rapidly than a larger area depending on the topographic characteristics (slope, vegetation and ground surface temperature, etc.) of the catchment. The snow cover extent was almost stable or increased slightly (Table 3) in all three catchments due to an increase, although statistically non-significant, in winter precipitation in the area. The slightly positive (statistically non-significant) trend in snow cover might be the reason for a positive mass balance of glaciers in the Central Karakoram region (Hunza) as reported by a number of investigators (Gardelle et al. 2012, 2013; Hewitt 2007; Kääb et al. 2012; Paul 2015; Rankl et al. 2014; Scherler et al. 2011). The increasing trend in snow cover (which was significant in the low-altitude zone and non-significant in the mid- and high-altitude zones) (Fig. 5; Table 3) in the Gilgit River basin was somewhat surprising because many studies (Berthier et al. 2007; Bolch et al. 2011; Gardelle et al. 2013; Kääb et al. 2015; Sarikaya et al. 2011; Vaughan et al. 2013) confirmed a negative mass balance in the glaciers of the Hindukush. This may be associated with the fact that the Gilgit River basin is situated in the extreme northern Hindukush range, bordering the Karakoram, and it

therefore has a climate that draws more from the climate of the Karakoram region (Hunza basin). Like the Karakoram ranges, the Gilgit basin undergoes an intrusion of Westerlies, such that winter precipitation trends in the Gilgit basin are similar to those of the Hunza basin (Fig. 1b). The moisture of the Westerlies is predominantly drained in the HKH region and little moisture is left in the far eastern and southern regions of the Himalayas.

The stable or marginally increasing snow cover trend in the Gilgit River basin was slightly stronger ($\tau = +0.33$) than in the Astore and Hunza River basins (Table 3) (at least at lower-altitude zones; Fig. 5). This difference was prominent in the snow accumulation ($\tau = +0.23$) and snowmelt ($\tau = +0.26$) periods (not significant for Gilgit). This might be associated with the declining trend in the mean summer temperature in the Gilgit River basin, as observed in Fig. 6, whereas the mean summer temperature trend was constant in the Hunza basin, as analyzed by Tahir et al. (2011). These results confirmed previous studies that showed that many regions within the UIB are undergoing glacier advance/stability, precipitation increase and mean temperature decrease (Archer and Fowler 2004; Bookhagen and Burbank 2010; Hewitt 1998, 2005, 2007; Scherler et al. 2011; Tahir et al. 2011, 2015).

5.2 Hydrological regime

Mean annual runoff from the Gilgit catchment, ≈ 712 mm, was lower or comparable with respect to the mean annual runoff generated from the Astore and Hunza basins; ≈ 1084 and ≈ 759 mm respectively (Table 3). This was consistent with the observed total annual precipitation values, which were lower in the Gilgit River basin than in the Astore and Hunza River basins (Table 3). The main source of runoff in all three river basins is winter snow-pack, which starts melting in the spring season (Fig. 4) and generates runoff.

The correlation results indicated that the annual discharge of the Gilgit River is influenced by the mean annual temperatures and the preceding winter precipitation as well as by the annual and seasonal snowmelt (Table 3). The correlation between summer discharge and summer mean temperature ($r = +0.65$) in the Gilgit River basin was somewhat lower than in the Hunza basin ($r = +0.81$) but higher than in the Astore River basin (Table 3). Summer stream flow in the Gilgit, Astore and Hunza basins was also positively correlated ($r = +0.48$, $+0.76$ and $+0.10$, respectively; non-significant) to the preceding winter's precipitation (winter snowfall) (Table 3), which melts in summer. A correlation analysis between the annual discharge and current summer precipitation indicated a weaker (non-significant) correlation in the Gilgit ($r = -0.3$), Astore ($r = +0.19$) and Hunza ($r = +0.005$)

River basins, which signified a minimal effect of summer monsoon rain in the Hindukush, central Karakoram and Western Himalaya regions. These differences might have also stemmed from the scarcity of precipitation data at high altitudes in these three sub-catchments of the UIB.

Overall, this study found significant correlation between the annual discharge, temperature and snow covered area change (Table 3) in the Gilgit, Astore and Hunza River basins. This indicated that UIB flow depends mainly on the snow melt, as reported by Mukhopadhyay and Khan (2014a), and is overlapped by the glacier melt rate, as indicated by Archer (2003) and Mukhopadhyay and Khan (2014a), which increases with the region's temperature seasonality (increased temperatures in spring and summer). This is in accordance with the results found by Mukhopadhyay and Khan (2014a) and Bookhagen and Burbank (2010), who showed that the total annual discharge of the Western Himalayan catchments (e.g., the Upper Indus Basin) are fed by snowmelt (up to $\approx 50\%$ of total discharge) and glacial melt (up to 21 % of total annual discharge).

6 Conclusions

A comparative assessment of the spatial extent of snow cover and the hydrological regime of the Gilgit, Astore and Hunza River basins (western, southern and northern parts of the UIB, respectively) were analyzed using remote sensing satellite data and ground station observations and the following conclusions were drawn:

1. A stable or slightly increasing trend in snow cover was found in the UIB in its western (Hindukush–Karakoram), southern (Western Himalaya) and northern (Central Karakoram) portions, possibly due to the offset effects of a positive (although statistically non-significant) trend in winter precipitation and a negative or constant summer temperature trend. This trend can be illustrated more confidently by replicating the analysis in the other sub-catchments of the UIB. A limited amount of data (15 years to present) for the MODIS time series is available, and longer records would help to draw robust conclusions on snow cover changes; nevertheless an important picture of the last decades' snow cover characteristics is provided by the current analysis.
2. Trend analyses, calculated over 29- and 62-year periods of hydrological and meteorological variables, respectively, suggested a non-significant, increasing trend in stream flow and seasonal (winter and summer) precipitation and a significant, decreasing trend in the summer mean temperature in the Gilgit River basin.
3. The discharge from the UIB depends much more on snow and glacier melt than on the rainfall-runoff in the western (Gilgit), southern (Astore) and northern portions (Hunza) of the UIB.

A thorough understanding of the complicated hydroclimatic conditions within the UIB may be facilitated by similar detailed studies of the other sub-catchments (e.g., Shigar, Shyok and Shingo River basins). A long time series of climatic data from high altitudes >3000 m ASL would be useful in detecting the hydroclimatic trends of the UIB more precisely. This can ultimately facilitate the transition to more effective and sustainable water resources management for the region (Halbe et al. 2013).

References

Akhtar M, Ahmad N, Booij MJ (2008) The impact of climate change on the water resources of Hindukush–Karakorum–Himalaya region under different glacier coverage scenarios. J Hydrol 355:148–163. doi:10.1016/j.jhydrol.2008.03.015

Araghi A, Adamowski J, Nalley D, Malard J (2015) Using wavelet transforms to estimate surface temperature trends and dominant periodicities in Iran based on gridded reanalysis data. J Atmos Res 11:52–72

Arendt A et al (2015) Randolph glacier inventory—a dataset of global glacier outlines: version 5.0. Global Land Ice Measurements from Space, Boulder Colorado, USA. Digital Media

Archer D (2003) Contrasting hydrological regimes in the upper Indus Basin. J Hydrol 274:198–210. doi:10.1016/S0022-1694(02)00414-6

Archer D (2004) Hydrological implications of spatial and altitudinal variation in temperature in the upper Indus basin. Nord Hydrol 35:209–222

Archer DR, Fowler HJ (2004) Spatial and temporal variations in precipitation in the Upper Indus Basin, global teleconnections and hydrological implications. Hydrol Earth Syst Sci 8:47–61. doi:10.5194/hess-8-47-2004

Archer DR, Forsythe N, Fowler HJ, Shah SM (2010) Sustainability of water resources management in the Indus Basin under changing climatic and socio economic conditions. Hydrol Earth Syst Sci HESS 14:1669–1680. doi:10.5194/hess-14-1669-2010

Berthier E, Arnaud Y, Kumar R, Ahmad S, Wagnon P, Chevallier P (2007) Remote sensing estimates of glacier mass balances in the Himachal Pradesh (Western Himalaya, India). Remote Sens Environ 108:327–338. doi:10.1016/j.rse.2006.11.017

Bolch T, Pieczonka T, Benn DI (2011) Multi-decadal mass loss of glaciers in the Everest area (Nepal Himalaya) derived from stereo imagery. Cryosphere 5:349–358. doi:10.5194/tc-5-349-2011

Bookhagen B, Burbank DW (2006) Topography, relief, and TRMM-derived rainfall variations along the Himalaya. Geophys Res Lett 33:L08405. doi:10.1029/2006GL026037

Bookhagen B, Burbank DW (2010) Toward a complete Himalayan hydrological budget: spatiotemporal distribution of snowmelt and rainfall and their impact on river discharge. J Geophys Res 115:F03019. doi:10.1029/2009JF001426

Dimri AP, Chevuturi A (2014) Model sensitivity analysis study for western disturbances over the Himalayas. Meteorol Atmos Phys 123:155–180. doi:10.1007/s00703-013-0302-4

Dimri AP, Yasunari T, Wiltshire A, Kumar P, Mathison C, Ridley J, Jacob D (2013) Application of regional climate models to the Indian winter monsoon over the western Himalayas. Sci Total Environ 468–469(Supplement):S36–S47. doi:10.1016/j.scitotenv.2013.01.040

Førland EJ et al (1996) Manual for operational correction of Nordic precipitation data. DNMI, Oslo

Forsythe N, Fowler H, Kilsby C, Archer D (2012a) Opportunities from remote sensing for supporting water resources management in village/valley scale catchments in the Upper Indus Basin. Water Resour Manag 26:845–871. doi:10.1007/s11269-011-9933-8

Forsythe N, Kilsby CG, Fowler HJ, Archer DR (2012b) Assessment of runoff sensitivity in the Upper Indus Basin to interannual climate variability and potential change using MODIS satellite data products. Mt Res Dev 32:16–29

Fowler HJ, Archer DR (2005) Hydro-climatological variability in the Upper Indus Basin and implications for water resources. In: Regional hydrological impacts of climatic change—impact assessment and decision making, Seventh IAHS Scientific Assembly at Foz do Iguaçu, Brazil, pp 131–138

Fowler HJ, Archer DR (2006) Conflicting signals of climatic change in the Upper Indus Basin. J Clim 19:4276–4293

Gardelle J, Berthier E, Arnaud Y (2012) Slight mass gain of Karakoram glaciers in the early twenty-first century. Nat Geosci 5:322–325. doi:10.1038/ngeo1450

Gardelle J, Berthier E, Arnaud Y, Kääb A (2013) Region-wide glacier mass balances over the Pamir-Karakoram-Himalaya during 1999–2011. Cryosphere 7:1263–1268. doi:10.5194/tc-7-1263-2013

Gilbert RO (1987) 16.5 Sen's nonparametric estimator of slope. In: Statistical methods for environmental pollution monitoring. Wiley, New York, p 217–219

Guo W et al (2015) The second Chinese glacier inventory: data, methods and results. J Glaciol 61:357–372

Gupta RP, Haritashya UK, Singh P (2005) Mapping dry/wet snow cover in the Indian Himalayas using IRS multispectral imagery. Remote Sens Environ 97:458–469. doi:10.1016/j.rse.2005.05.010

Halbe J, Pahl-Wostl C, Sendzimir J, Adamowski J (2013) Towards adaptive and integrated management paradigms to meet the challenges of water governance. Water Sci Tech Water Supply 67:2651–2660

Hall DK, Riggs GA (2007) Accuracy assessment of the MODIS snow products. Hydrol Process 21:1534–1547. doi:10.1002/hyp.6715

Hall D, Riggs G, Salomonson VV (2006) MODIS/Terra Snow Cover 8-day L3 Global 500 m Grid V005, [March 2000 to December 2012]. National Snow and Ice Data Center, Boulder. Digital media. http://nsidc.org/data/mod10a2v5.html. Accessed 15 Jan 2013

Hartmann DL et al (2013) Observations: atmosphere and surface. In: Stocker TF, Qin D, Plattner GK, Tignor M, Allen SK, Boschung

J, Nauels A, Xia Y, Bex V, Midgley PM (eds) Climate change 2013: the physical science basis. Contribution of Working Group I to the fifth assessment report of the intergovernmental panel on climate change. Cambridge University Press, Cambridge

Hasson S, Lucarini V, Khan MR, Petitta M, Bolch T, Gioli G (2014) Early 21st century snow cover state over the western river basins of the Indus River system. Hydrol Earth Syst Sci 18:4077–4100. doi:10.5194/hess-18-4077-2014

Hewitt K (1998) Glaciers receive a surge of attention in the Karakoram Himalaya. EOS Trans Am Geophys Union 79:104–105

Hewitt K (2005) The Karakoram anomaly? Glacier expansion and the elevation effect, Karakoram Himalaya. Mt Res Dev 25:332–340

Hewitt K (2007) Tributary glacier surges: an exceptional concentration at Panmah Glacier, Karakoram Himalaya. J Glaciol 53:181–188

Hewitt K, Wake CP, Young GJ, David C (1989) Hydrological Investigation at Biafo Glacier, Karakoram Range, Himalaya; an important source of water for the Indus River. Ann Glaciol 13:103–108

Hirsch RM, Slack JR (1984) A nonparametric trend test for seasonal data with serial dependence. Water Resour Res 20:727–732

Hirsch RM, Slack JR, Smith RA (1982) Techniques of trend analysis for monthly water quality data. Water Resour Res 18:107–121

Immerzeel WW, Droogers P, de Jong SM, Bierkens MFP (2009) Large-scale monitoring of snow cover and runoff simulation in Himalayan river basins using remote sensing. Remote Sens Environ 113:40–49. doi:10.1016/j.rse.2008.08.010

Immerzeel WW, Pellicciotti F, Shrestha AB (2012) Glaciers as a proxy to quantify the spatial distribution of precipitation in the Hunza Basin. Mt Res Dev 32:30–38

Immerzeel WW, Pellicciotti F, Bierkens MFP (2013) Rising river flows throughout the twenty-first century in two Himalayan glacierized watersheds. Nat Geosci 6:742–745. doi:10.1038/ngeo1896

Immerzeel WW, Wanders N, Lutz AF, Shea JM, Bierkens MFP (2015) Reconciling high-altitude precipitation in the upper Indus basin with glacier mass balances and runoff. Hydrol Earth Syst Sci 19:4673–4687. doi:10.5194/hess-19-4673-2015

Kääb A, Berthier E, Nuth C, Gardelle J, Arnaud Y (2012) Contrasting patterns of early twenty-first-century glacier mass change in the Himalayas. Nature 488:495–498. doi:10.1038/nature11324

Kääb A, Treichler D, Nuth C, Berthier E (2015) Brief communication: contending estimates of 2003–2008 glacier mass balance over the Pamir-Karakoram-Himalaya. The Cryosphere 9:557–564. doi:10.5194/tc-9-557-2015

Kendall MG (1975) Rank correlation measures, 4th edn. Charles Griffin, London

Kendall MG, Gibbons JD (1990) Rank correlation methods, 5th edn. Edward Arnold, London

Khan A, Naz BS, Bowling LC (2015) Separating snow, clean and debris covered ice in the Upper Indus Basin, Hindukush-Karakoram-Himalayas, using Landsat images between 1998 and 2002. J Hydrol 521:46–64. doi:10.1016/j.jhydrol.2014.11.048

Lee S, Klein AG, Over TM (2005) A comparison of MODIS and NOHRSC snow-cover products for simulating streamflow using the Snowmelt Runoff Model. Hydrol Process 19:2951–2972. doi:10.1002/hyp.5810

Liniger H, Weingartner R, Grosjean M (eds) (1998) Mountains of the world: Water towers for the 21st century. Mountain agenda for the commission on sustainable development (CSD), BO12, Berne

Mann HB (1945) Nonparametric tests against trend. Econometrica 13:245–259

Maurer EP, Rhoads JD, Dubayah RO, Lettenmaier DP (2003) Evaluation of the snow-covered area data product from MODIS. Hydrol Process 17:59–71. doi:10.1002/hyp.1193

METI, NASA (2011) ASTER Global Digital Elevation Model (GDEM) version 2, vol 2013. http://reverb.echo.nasa.gov/reverb/. Accessed 15 Nov 2015

Mukhopadhyay B, Khan A (2014a) A quantitative assessment of the genetic sources of the hydrologic flow regimes in Upper Indus Basin and its significance in a changing climate. J Hydrol 509:549–572. doi:10.1016/j.jhydrol.2013.11.059

Mukhopadhyay B, Khan A (2014b) Rising river flows and glacial mass balance in central Karakoram. J Hydrol 513:192–203. doi:10.1016/j.jhydrol.2014.03.042

Mukhopadhyay B, Khan A (2015) A reevaluation of the snowmelt and glacial melt in river flows within Upper Indus Basin and its significance in a changing climate. J Hydrol. doi:10.1016/j.jhydrol.2015.04.045

Nalley D, Adamowski J, Khalil B (2012) Using discrete wavelet transforms to analyze trends in streamflow and precipitation in Quebec and Ontario (1954–2008). J Hydrol 475:204–228

Nalley D, Adamowski J, Khalil B, Ozga-Zielinski B (2013) Trend detection in surface air temperature in Ontario and Quebec, Canada during 1967–2006 using the discrete wavelet transform. J Atmos Res 132/133:375–398

Nuimura T et al (2015) The GAMDAM glacier inventory: a quality-controlled inventory of Asian glaciers. Cryosphere 9:849–864. doi:10.5194/tc-9-849-2015

Paul F (2015) Revealing glacier flow and surge dynamics from animated satellite image sequences: examples from the Karakoram. Cryosphere 9:2201–2214. doi:10.5194/tc-9-2201-2015

Pellicciotti F, Bauder A, Parola M (2010) Effect of glaciers on streamflow trends in the Swiss Alps. Water Resour Res 46:W10522. doi:10.1029/2009wr009039

Pingale S, Khare D, Jat M, Adamowski J (2014) Spatial and temporal trends of mean and extreme rainfall and temperature for the 33 urban centres of the arid and semi-arid state of Rajasthan, India. J Atmos Res 138:73–90

Ragettli S et al (2015) Unraveling the hydrology of a Himalayan catchment through integration of high resolution in situ data and remote sensing with an advanced simulation model. Adv Water Res 78:94–111. doi:10.1016/j.advwatres.2015.01.013

Rankl M, Kienholz C, Braun M (2014) Glacier changes in the Karakoram region mapped by multimission satellite imagery. Cryosphere 8:977–989. doi:10.5194/tc-8-977-2014

Ridley J, Wiltshire A, Mathison C (2013) More frequent occurrence of westerly disturbances in Karakoram up to 2100. Sci Total Environ 468–469(Supplement):S31–S35. doi:10.1016/j.scitotenv.2013.03.074

Rodgers JL, Nicewander WA (1988) Thirteen ways to look at the correlation coefficient. Am Stat 42:59–66

Sarikaya MA, Bishop MP, Shroder JF, Olsenholler JA (2011) Space-based observations of Eastern Hindu Kush glaciers between 1976 and 2007, Afghanistan and Pakistan. Remote Sens Lett 3:77–84. doi:10.1080/01431161.2010.536181

Savéan M et al (2015) Water budget on the Dudh Koshi River (Nepal): uncertainties on precipitation. J Hydrol. doi:10.1016/j.jhydrol.2015.10.040

Scherler D, Bookhagen B, Strecker MR (2011) Spatially variable response of Himalayan glaciers to climate change affected by debris cover. Nat Geosci 4:156–159. doi:10.1038/NGEO1068

Sen PK (1968) Estimates of the regression coefficient based on Kendall's tau. J Am Stat Assoc 63:1379–1389. doi:10.1080/01621459.1968.10480934

Sevruk B (1985) Correction of precipitation measurements. In: Workshop on the correction of precipitation measurements, WMO/IAHS/ETH, Zurich, Switzerland, p 13–23

Sevruk B (1989) Reliability of precipitation measurement. In: International workshop on precipitation measurement, WMO Tech Document, pp 13–19

SIHP (1990) Snow and ice hydrology project. WAPDA-IDRC-Wilfrid Laurier University, Upper Indus river basin

Sirguey P, Mathieu R, Arnaud Y, Fitzharris BB (2009) Seven years of snow cover monitoring with MODIS to model catchment discharge in New Zealand. Paper presented at the IEEE international geoscience and remote sensing symposium (IGARSS), Cape Town, 12–17 July 2009

Spearman C (1904) The proof and measurement of association between two things. Am J Psychol 15:72–101

Tahir AA, Chevallier P, Arnaud Y, Ahmad B (2011) Snow cover dynamics and hydrological regime of the Hunza River basin, Karakoram Range, Northern Pakistan. Hydrol Earth Syst Sci HESS 15:2275–2290. doi:10.5194/hess-15-2275-2011

Tahir AA, Chevallier P, Arnaud Y, Ashraf M, Bhatti MT (2015) Snow cover trend and hydrological characteristics of the Astore River basin (Western Himalayas) and its comparison to the Hunza basin (Karakoram region). Sci Total Environ 505:748–761. doi:10.1016/j.scitotenv.2014.10.065

Tekeli AE, Akyürek Z, Arda Sorman A, Sensoy A, Ünal Sorman A (2005) Using MODIS snow cover maps in modeling snowmelt runoff process in the eastern part of Turkey. Remote Sens Environ 97:216–230

Treydte KS, Schleser GH, Helle G, Frank DC, Winiger M, Haug GH, Esper J (2006) The twentieth century was the wettest period in northern Pakistan over the past millennium. Nature 440:1179–1182. doi:10.1038/nature04743

Vauchel P (2005) Hydraccess 4.2 edn. Institute of Research for Development, France

Vaughan DG et al (2013) Observations: cryosphere. In: Stocker TF, Qin D, Plattner GK, Tignor M, Allen SK, Boschung J, Nauels A, Xia Y, Bex V, Midgley PM (eds) Climate change 2013: the physical science basis. Contribution of Working Group I to the fifth assessment report of the intergovernmental panel on climate change, Cambridge University Press, Cambridge

Wake CP (1989) Glaciochemical investigations as a tool to determine the spatial variation of snow accumulation in the Central Karakoram, Northern Pakistan. Ann Glaciol 13:279–284

Wang X, Xie H, Liang T (2008) Evaluation of MODIS snow cover and cloud mask and its application in Northern Xinjiang, China. Remote Sens Environ 112:1497–1513. doi:10.1016/j.rse.2007.05.016

Young GJ, Hewitt K (1990) Hydrology research in the upper Indus basin, Karakoram Himalaya, Pakistan. In: Hydrology of mountainous areas, Czechoslovakia, International Association Hydrological Sciences, p 139–152